

In Situ Photoconversion of Multicolor Luminescence and Pure White Light Emission Based on Carbon Dot-Supported Supramolecular Assembly

Huang Wu,^{‡,†} Yong Chen,[‡] Xianyin Dai,[‡] Peiyu Li,[‡] J. Fraser Stoddart,^{*,†,‡,⊥,||} and Yu Liu^{*,‡,§}

[‡]College of Chemistry, State Key Laboratory of Elemento-Organic Chemistry, Nankai University, 94 Weijin Road, Nankai District, Tianjin 300071, P.R. China

[†]Department of Chemistry, Northwestern University, 2145 Sheridan Road, Evanston, Illinois 60208, United States

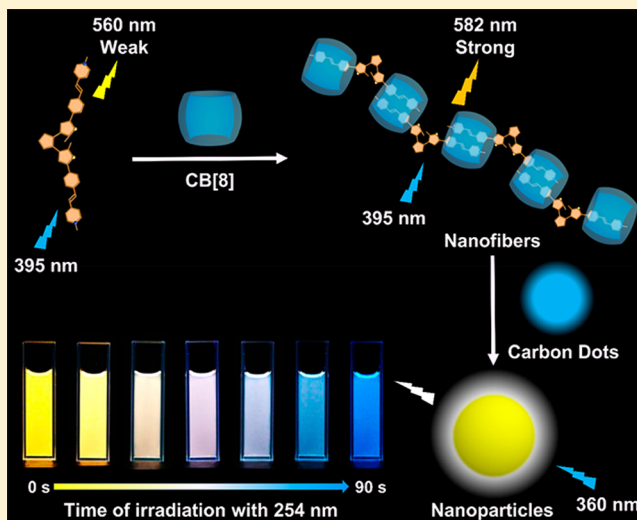
[⊥]School of Chemistry, University of New South Wales, Sydney, NSW 2052, Australia

^{||}Institute for Molecular Design and Synthesis, Tianjin University, 92 Weijin Road, Nankai District, Tianjin 300072, P.R. China

[§]Collaborative Innovation Center of Chemical Science and Engineering (Tianjin), 92 Weijin Road, Nankai District, Tianjin 300072, P. R. China

Supporting Information

ABSTRACT: Constructing multicolor photoluminescence materials that allow for the integration of suitable external stimuli in order to control luminescence color conversions is a challenging objective. Multicolor luminescent output that is regulated in an in situ photo-controlled manner is not a common phenomenon. Herein, a photoluminescent supramolecular assembly, prepared in two stages, is described that displays in situ photo-tuning broad-spectrum output. Benefiting from the reversible photo-switched constitutional interconversion of diarylethenes, the fluorescence of a guest molecule, styrylpyridinium-modified diarylethene, can be switched on/off by alternating ultraviolet and visible light irradiation. Upon complexation of this guest with a host, cucurbit[8]uril, the fluorescence intensity of the resulting binary supramolecular nanofiber shows a drastic enhancement when compared with that of the free guest, which can also be quenched and recovered reversibly by light irradiation. Significantly, such cationic supramolecular nanofibers also interact with anionic carbon dots to form broad-spectrum output ternary supramolecular assemblies, the fluorescence of which can be changed efficiently from yellow to blue in an in situ photo-controlled manner. Pure white light emission can be realized expediently in the luminescence color-conversion process. The use of light as an external stimulus to regulate fluorescent color conversion provides us with an opportunity to design and construct more advanced anti-counterfeiting materials as well as visual display instruments.



INTRODUCTION

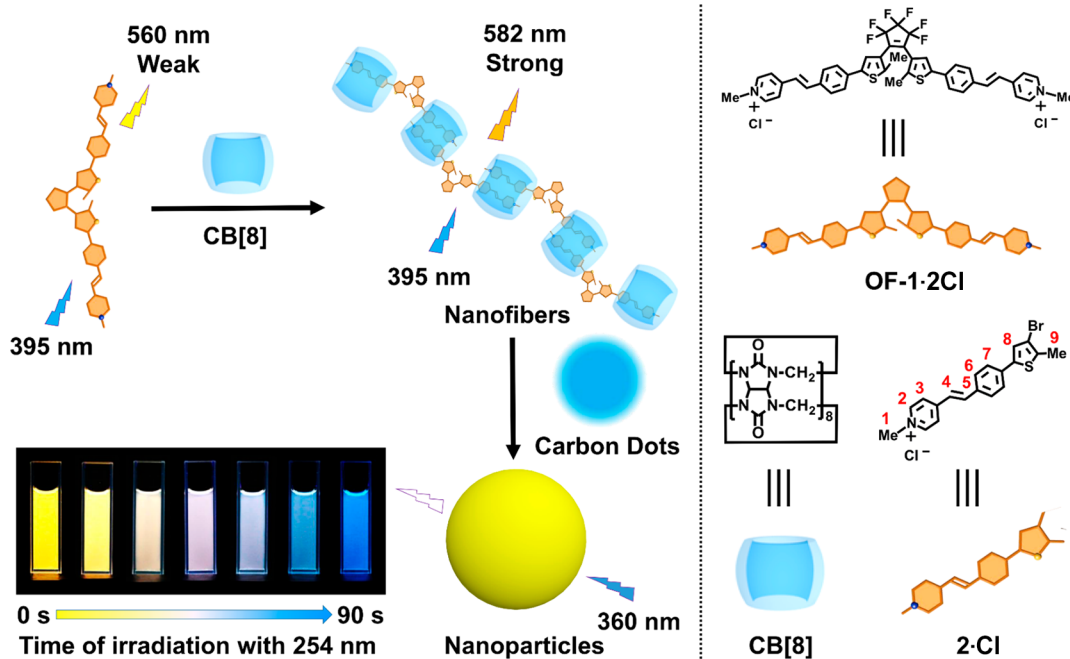
The construction of multicolor photoluminescence materials that can be tuned in a simple manner has attracted an increasing amount of attention¹ because of their potential applications as biological image reagents,² stretchable displays,³ multidimensional sensors,⁴ photoelectric devices,⁵ and light-emitting diodes.⁶ The conventional methods of acquiring such materials are mainly physical blending or the covalent connections of chromophores with complementary fluorescence in accurate ratios.⁷ Luminescent materials that can be tuned for white-light emission are particularly important, since they can be applied practically in the fields of visual display media and lighting instruments.⁸ Thus far, development of this

type of white-light emission material is limited by the available preparation protocols or device fabrication techniques.⁹ In contrast to the conventional approaches, several non-covalent strategies have been developed in recent years for the synthesis of multicolor emission materials that respond to external stimuli.¹⁰ For example, Yam et al.¹¹ have constructed a new class of amphiphilic anionic platinum(II) assemblies that display tunable fluorescence emission that can be tuned by variation of solvent polarity. Ito et al.¹² have reported a gold(I) isocyanide complex that exhibits different photoluminescent

Received: December 21, 2018

Published: March 12, 2019

Scheme 1. Schematic Illustration of the in Situ Photo-switched Multicolor Luminescence Supramolecular Assembly



colors interconvertibly by treatment with acetone and mechanical shearing in the solid state. Tian et al.¹³ have utilized two-armed fluorescent molecules as guests and γ -cyclodextrin as the host to construct novel host–guest complexes which show multicolor luminescence that relies on intramolecular charge transfer. Tao et al.¹⁴ have reported that various fluorescent emissions can be obtained by adjusting the electronic distributions of the *p*-phenylenevinylene units within the hydrophobic cavity of cucurbit[8]uril. The use of external stimuli to regulate multicolor luminescent output provides a convenient way to construct new classes of photoluminescent materials. Among these external stimuli, light is of particular interest because of its clean, non-invasive, and remote-controlling nature.¹⁵ Reports of such fluorescence color-conversion processes that can be regulated in a reversible photo-controlled manner are still rare.

Among the various building blocks¹⁶ for constructing photo-responsive supramolecular systems, diarylethene derivatives (DAEs), on account of their generally (i) rapid light response, (ii) absent spontaneous thermal reversion, and (iii) outstanding photochromic properties,¹⁷ have led to many successful applications as optical switches,¹⁸ molecular modulators,¹⁹ helical transfer controllers,²⁰ and information storage media.²¹ Meanwhile, carbon dots (CDs) are a popular class of carbon nanomaterials, with the promising advantages of non-toxicity, eco-friendliness, high fluorescence, biocompatibility, good water solubility, excellent photostability, and easy surface functionalization.²² CDs have been, therefore, widely utilized as photosensitizers,²³ imaging-guided nanocarriers,²⁴ multidimensional memory materials,²⁵ and biosensors.²⁶ In this investigation, a photo-responsive multicolor luminescent supramolecular assembly is constructed (Scheme 1) from anionic CDs and cationic supramolecular nanofibers that are composed of the styrylpyridinium-modified perfluorocyclopentene diarylethene derivative 1^{2+} and cucurbit[8]uril (CB[8]). On account of the reversible photoisomerization of the DAE unit, the fluorescence of styrylpyridinium-modified

DAE guest molecule 1^{2+} and the resulting binary supramolecular nanofibers $1^{2+}\text{CB}[8]$ can be switched on/off by alternating ultraviolet and visible light irradiation. Such photo-responsive cationic supramolecular nanofibers further co-assemble with the anionic CDs to form ternary supramolecular nanoparticles, which exhibit colorful emission capacities—i.e., gold, yellow, khaki, and blue—while the luminescent colors of the ternary supramolecular assembly can be interconverted efficiently by irradiation with ultraviolet and visible light. White light emission is also realized in the fluorescence color-conversion process.

RESULTS AND DISCUSSION

Synthetic routes to the guest molecules $1\cdot 2\text{Cl}/2\cdot\text{Cl}$ and CDs are summarized in Schemes S1 and S2, respectively. The guest molecule $1\cdot 2\text{Cl}$ is obtained in 78% yield by the condensation of the DAE derivative **6** with 4-picolinium iodide, followed by counterion exchanges. Employing a similar synthetic method, the reference compound $2\cdot\text{Cl}$, with better water solubility, is prepared in 88% yield. The CDs are prepared by means of thermal pyrolysis with citric acid as the carbon source and diethylenetriamine as the surface passivation agent, followed by amide condensation with succinic anhydride. The UV–vis absorption spectrum (Figure 1b) of the open-ring form (OF- 1^{2+}) of 1^{2+} shows a strong absorption peak at 395 nm. After irradiation of aqueous solutions of OF- 1^{2+} with UV light (254 nm, 2.0 min), the absorption peak at 395 nm decreases gradually with a blue shift of ~ 10 nm, accompanied by the appearance of a new absorption band centered on 625 nm. Three clear isosbestic points are observed at 311, 360, and 465 nm in the UV–vis absorption spectrum. The photocyclization quantum yield (Φ_{o-c}) for 1^{2+} is determined (Table S1) to be 0.30. In addition, color changes (Figure 1a) from pale yellow to blue are observed after UV light irradiation of an aqueous solution of 1^{2+} . These phenomena are attributed²⁷ to (Figure 1a) the transformation of 1^{2+} from the open-ring form (OF- 1^{2+}) to the closed-ring form (CF- 1^{2+}). When an aqueous

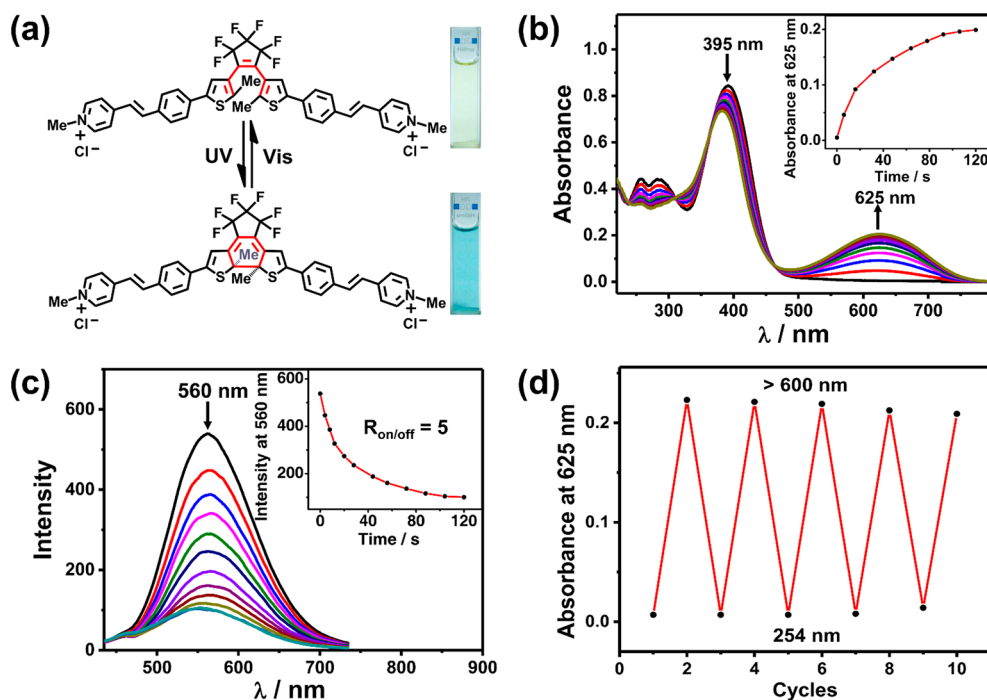


Figure 1. (a) Structural formulas and photographic images of the changes of 1^{2+} upon alternating irradiation with UV and visible light. (b) UV–vis absorption spectra and (inset) absorbance intensity changes of $OF-1^{2+}$ at 625 nm ($[OF-1^{2+}] = 2.0 \times 10^{-5}$ M, 298 K) upon irradiation with UV light (254 nm, 2.0 min). (c) Emission spectra and (inset) emission intensity changes of $OF-1^{2+}$ at 560 nm ($[OF-1^{2+}] = 5.0 \times 10^{-6}$ M, $\lambda_{ex} = 395$ nm, 298 K) upon irradiation with UV light (254 nm, 2.0 min). (d) Absorbance changes at 625 nm of 1^{2+} ($[1^{2+}] = 2.0 \times 10^{-5}$ M, 298 K) upon alternating irradiation with UV (254 nm, 2.0 min) and visible (>600 nm, 1.5 min) light in aqueous solutions.

solution of $CF-1^{2+}$ is irradiated with visible light (>600 nm, 1.5 min), the color of the $CF-1^{2+}$ solution returns to being pale yellow, and its UV–vis absorption spectrum almost resembles (Figure S8) that of $OF-1^{2+}$. When the solution is excited at 395 nm, the fluorescence spectrum of 1^{2+} reveals (Figure 1c) an emission peak centered on 560 nm. Upon irradiation of the solution with UV light (254 nm, 2.0 min), the fluorescence intensity of 1^{2+} is gradually quenched by 82%, and the fluorescence quantum yield of 1^{2+} decreases (Table S3) from 0.63% to 0.010% because of the self-absorption effect of $CF-1^{2+}$. The fluorescence on/off quenching ratio ($R_{on/off}$) is calculated to be 5 by comparing the intensity values at the maximum emission wavelength before and after UV light irradiation. When the aqueous solution is irradiated with visible light (>600 nm, 1.0 min), the fluorescence is recovered. These results indicate that the constitution of 1^{2+} can go back and forth between the open-ring and closed-ring isomers upon alternating irradiation with UV and visible light. The wavelength of the excitation light shows a negligible influence on the photoisomerization reaction of 1^{2+} under the current experimental conditions (Figure S12), but this influence is inevitable when using a high-intensity excitation light source (Figure S13). Moreover, this interconversion could be repeated (Figures 1d and S8) for several cycles without appreciable light fatigue. The ring-closing conversion yield of 1^{2+} is measured (Figure S11a) to be 79% upon irradiation with UV light. Furthermore, $CF-1^{2+}$ can return quantitatively to $OF-1^{2+}$ upon irradiation (Figure S11b) with visible light. All these results demonstrate the excellent photo-switched constitutional interconversion of 1^{2+} .

Cucurbit[8]uril (CB[8]),²⁸ which possesses high binding affinity toward a variety of neutral or cationic guest molecules, has been used widely as the assembler of supramolecular

architectures in aqueous solutions. It can therefore be anticipated that CB[8] will bind to positively charged 1^{2+} . The supramolecular assembly consisting of 1^{2+} and CB[8] was studied by UV–vis absorption, NMR, and fluorescence spectroscopies. Upon stepwise addition of CB[8] to an aqueous solution of $OF-1^{2+}$, the absorption peak of 1^{2+} centered on 395 nm shifts gradually (Figure S14) to 420 nm. The binding constant K_a between $OF-1^{2+}$ and CB[8] is determined (Figure S14, inset) to be 1.19×10^7 M⁻¹ in aqueous solutions. A Job plot shows (Figure S15) a maximum at a molar fraction of 0.5, indicating a 1:1 stoichiometric ratio between $OF-1^{2+}$ and CB[8]. On account of the high affinity between CB[8] and $OF-1^{2+}$, supramolecular nanofibers are obtained readily. Transmission electron microscopy (TEM, Figure 2b) and atomic force microscopy (AFM, Figure S16) images reveal one-dimensional (1D) fine nanofibers with lengths of several micrometers. The average hydrodynamic diameter has been determined (Figure S17) to be 470 nm upon equimolar mixing of CB[8] and 1^{2+} , indicating the formation of highly polymerized supramolecular assemblies. In order to verify the binding mode of CB[8] with 1^{2+} , reference compound 2^+ with better water-solubility was synthesized (Figures S5–S7). In the ¹H NMR spectrum (Figure S18) of a 2:1 mixture of 2^+ and CB[8], the chemical shifts of the protons (H_4 and H_5) residing on the C=C double bonds and those (H_6 and H_7) residing on the phenylene groups show upfield shifts ($\Delta\delta = 0.45, 0.42, 0.64,$ and 0.30 ppm for $H_4, H_5, H_6,$ and H_7 , respectively). The resonances of the protons ($H_1, H_2,$ and H_3) residing on the pyridinium rings and those (H_8 and H_9) on the thiophene rings are shifted downfield ($\Delta\delta = 0.03$ – 0.22 ppm). In addition, correlation peaks are observed (Figure S19) between pyridinium protons ($H_1, H_2,$ and H_3) and thiophene protons (H_8 and H_9) in the two-dimensional (2D) ROESY

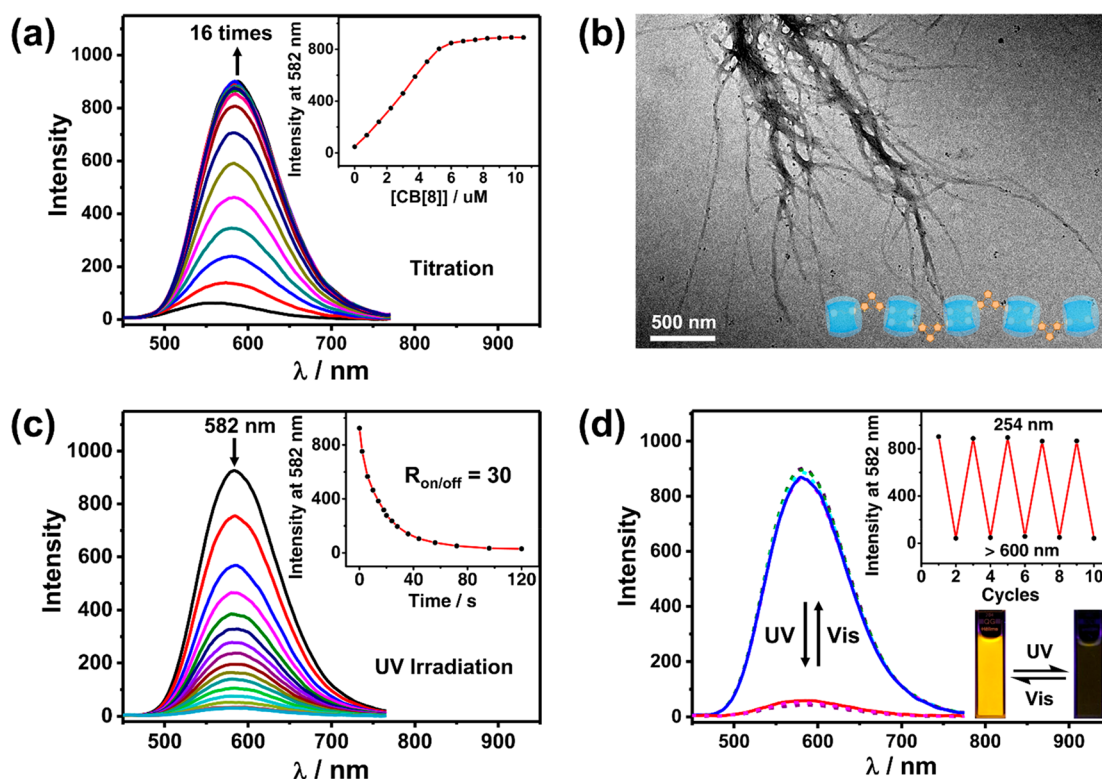


Figure 2. (a) Emission spectra and (inset) emission intensity changes of OF-1^{2+} at 582 nm ($[\text{OF-1}^{2+}] = 5.0 \times 10^{-6}$ M, $[\text{CB}[8]] = 0\text{--}10.5 \times 10^{-6}$ M, $\lambda_{\text{ex}} = 395$ nm, 298 K) upon gradual addition of CB[8] in an aqueous solution. (b) TEM image of $\text{OF-1}^{2+}\text{@CB}[8]$ supramolecular assembly. (c) Emission spectra and (inset) emission intensity changes of $\text{OF-1}^{2+}\text{@CB}[8]$ at 582 nm ($[\text{OF-1}^{2+}\text{@CB}[8]] = 5.0 \times 10^{-6}$ M, $\lambda_{\text{ex}} = 395$ nm, 298 K) upon irradiation with UV light (254 nm, 2.0 min). (d) Emission spectra and (inset) emission intensity changes of $\text{OF-1}^{2+}\text{@CB}[8]$ at 582 nm ($[\text{OF-1}^{2+}\text{@CB}[8]] = 5.0 \times 10^{-6}$ M, $\lambda_{\text{ex}} = 395$ nm, 298 K) upon alternating irradiation with UV (254 nm, 2.0 min) and visible light (>600 nm, 40 s) in an aqueous solution.

spectrum. Combining the 1D and 2D NMR spectra, it is clear that CB[8] is bound to the phenylene and C=C double bond units. Considering the intermolecular steric effect between the pyridinium and perfluorocyclopentene units in the binary supramolecular assembly $\text{OF-1}^{2+}\text{@CB}[8]$, the bonding mode of $\text{OF-1}^{2+}\text{@CB}[8]$ was confirmed by theoretical calculations using the unilateral styrylpyridinium-modified DAE (3^+) as a model compound. The energy-optimized structure for the $\text{OF-3}^+\text{@CB}[8]$ was determined to be that (Figure S20 and Table S2) in which the phenylene group and C=C double bond units are included in the cavity of CB[8], which is in agreement with the result from ^1H NMR spectroscopy.

Upon complexation with CB[8], the fluorescence intensity of OF-1^{2+} increases (Figure 2a) 16-fold as compared to the inherent fluorescence of OF-1^{2+} , benefiting from the fact that free rotation of the C=C double bond is restricted by CB[8].²⁹ The fluorescence quantum yield of $\text{OF-1}^{2+}\text{@CB}[8]$ was measured to be 12% (Table S3), a value which is considerably higher than that (0.63%) for free OF-1^{2+} . The maximum emission wavelength is shifted bathochromically from 560 to 582 nm as a result of the J-stacking of styrylpyridinium units in the cavity of CB[8].^{14,30} Furthermore, upon irradiation with the UV light (254 nm, 2.0 min), the fluorescence intensity of $\text{1}^{2+}\text{@CB}[8]$ is quenched (Figure 2c) gradually by 97%. The fluorescent on/off quenching ratio ($R_{\text{on/off}}$) was calculated to be 30. The fluorescence quenching can also be detected by the naked eye, wherein the bright yellow fluorescence of the $\text{OF-1}^{2+}\text{@CB}[8]$ gradually turns dark (Figure 2d, inset) upon irradiation with UV light. When the

non-luminous aqueous solution is irradiated with visible light (>600 nm, 40 s), the yellow fluorescence recovers (Figure 2d, inset). These results indicate that the constitutions of 1^{2+} can also be interconverted between OF-1^{2+} and CF-1^{2+} in the host-guest complex upon light irradiation. The UV-vis absorption spectra also confirm the outstanding photo-conversion cycles of $\text{1}^{2+}\text{@CB}[8]$. Upon irradiation of aqueous solutions of $\text{OF-1}^{2+}\text{@CB}[8]$ with UV light (254 nm, 2.0 min), the strong absorption peak at 420 nm decreases gradually (Figure S21) and a new absorption peak appears at 655 nm with a 30 nm bathochromic shift compared with that (625 nm) of 1^{2+} . The UV-vis absorption spectrum reverts back to its original state upon visible light irradiation (>600 nm, 1.0 min). These processes can be repeated (Figure S22) through several cycles without appreciable light fatigue, an observation which is consistent (Figure 2d) with the fluorescence spectra.

In order to utilize fully the photo-switched fluorescence behavior of the present cationic supramolecular assembly $\text{1}^{2+}\text{@CB}[8]$, CDs are employed as a model substrate in the construction of a broad-spectrum output luminescent supramolecular material. There are two inherent advantages of introducing CDs into the $\text{1}^{2+}\text{@CB}[8]$ supramolecular assembly: (1) CDs emit bright blue fluorescence, which is complemented by the yellow fluorescence of the supramolecular nanofiber²⁵ $\text{1}^{2+}\text{@CB}[8]$. (2) The spherical distribution of charged functional groups on the surface of CDs provides an ideal adhesion agent to promote the co-assembly with the cationic supramolecular nanofiber, $\text{1}^{2+}\text{@CB}[8]$. Experimentally, CDs are prepared by thermal pyrolysis, and

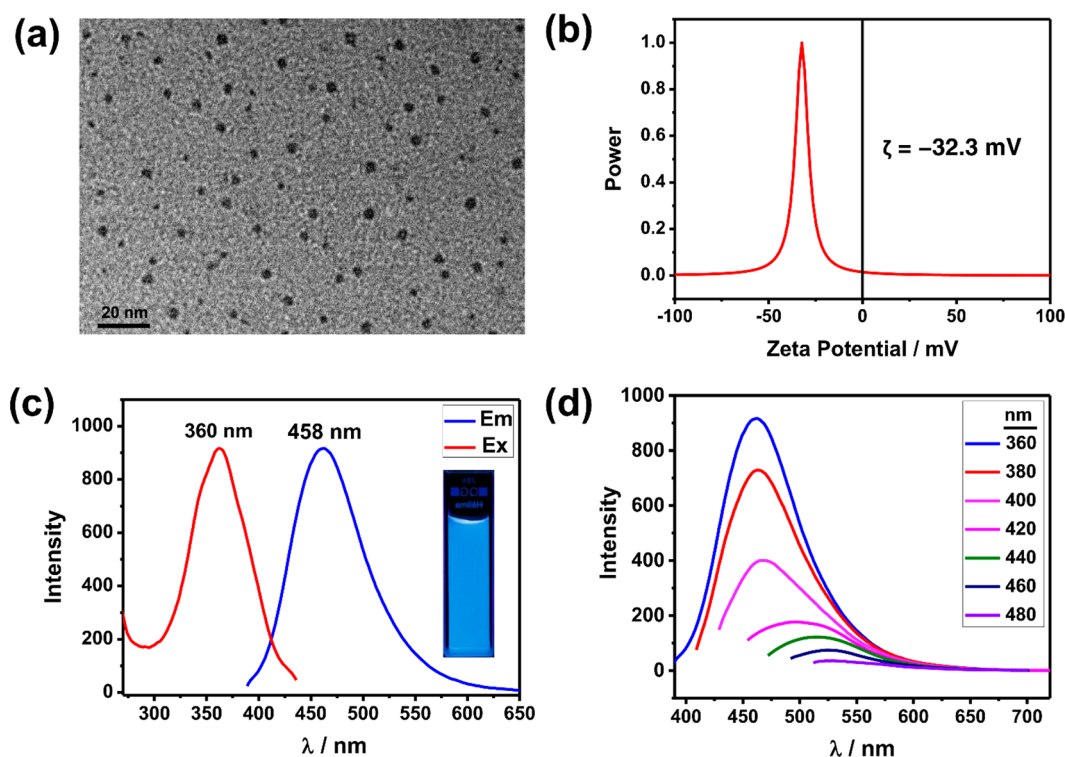


Figure 3. (a) TEM image of the anionic CDs. (b) Zeta potential of the anionic CDs in a neutral aqueous solution. (c) Excitation and emission spectra of the anionic CDs ($[CDs] = 3 \mu\text{g/mL}$, 298 K). (d) Emission spectra of the anionic CDs ($[CDs] = 3 \mu\text{g/mL}$, 298 K) at various excitation wavelengths in a neutral aqueous solution.

their morphology is investigated by TEM. A number of black dots with a size distribution of 4–8 nm are observed in the TEM image (Figure 3a). The average hydrated radius is 5.5 nm (Figure S23). The high-resolution TEM analysis reveals (Figure S24) the lattice spacings of CDs to be 0.39 and 0.22 nm, corresponding to the diffraction peaks (Figure S25) centered on 40.2° and 22.5° in the powder X-ray diffraction pattern, respectively. This result indicates that the CDs are highly crystalline.³¹ The UV–vis absorption spectrum of the CDs exhibits (Figure S26a) two absorption peaks, at 260 and 360 nm, which can be assigned³² to the π – π^* transitions of the aromatic ring components and the n – π^* transition of the C=O group on the surface of CDs, respectively. When the CDs are excited at 360 nm, strong blue fluorescence is observed (Figure 3c, inset). The fluorescence spectrum reveals (Figure 3c) an emission peak centered on 458 nm, and the corresponding fluorescence quantum yield (Table S3) is 31%. The fluorescence spectra of the CDs are excitation wavelength- and pH-dependent. The emission peaks are shifted (Figure 3d) bathochromically from 458 to 537 nm when the excitation wavelengths are changed from 360 to 480 nm. The fluorescence intensity increases (Figure S26b) progressively with a change in pH from 2 to 7. There are no obvious changes in fluorescence intensity upon further enhancing the basicity. The functional groups on the surface of the CDs have been studied by Fourier transform infrared (FTIR) spectroscopy and X-ray photoelectron spectroscopy (XPS). The broad vibrational bands in the range of 3000–3500 cm^{-1} can be assigned to O–H and N–H stretching vibrations. The vibration bands at 1633, 1550, 1417, and 1259 cm^{-1} can be ascribed to the stretching vibration of C=O, the bending vibration of N–H, and the stretching vibrations of C–N and C–O, respectively (Figure S27). The XPS spectrum

shows (Figure S28) strong signal peaks for the elements C, O, and N. These results demonstrate that there are many carboxylic acids and amide groups distributed on the surface of the CDs. In addition, the zeta potentials of the CDs decrease (Figure S29) gradually from 30.6 to -48.1 mV when the pH is changed from 2 to 9. In a neutral aqueous solution, the zeta potential of the CDs (Figure 3b) is -32.3 mV, indicating that the carboxylic acids are the dominant functional groups on the surface of the CDs.

On account of the good luminescence behavior and the anionic surface functional groups of the CDs, the luminescent supramolecular assembly $CDs@I^{2+}CB[8]$ can be readily constructed by electrostatic interactions between the cationic supramolecular nanofibers $I^{2+}CB[8]$ and the anionic CDs. The scanning electron microscopy (SEM) image of the supramolecular assembly $CDs@I^{2+}CB[8]$ shows (Figure S30b) numerous spherical nanoparticles with an average diameter of ~ 700 nm, consistent with the features observed (Figure S30a) in the TEM image. A dynamic light scattering (DLS) experiment reveals (Figure S31) the average hydrodynamic diameter of the $CDs@I^{2+}CB[8]$ nanoparticles to be 757 nm in neutral aqueous solution. In addition, the zeta potential of $CDs@I^{2+}CB[8]$ supramolecular nanoparticles was determined (Figure S32) to be -16.9 mV, a value which is higher than that (-32.3 mV) of CDs. All of these results demonstrate consistently that the cationic $I^{2+}CB[8]$ supramolecular nanofibers are able to co-assemble efficiently with the anionic CDs, courtesy of electrostatic interactions. $CDs@OF-I^{2+}CB[8]$ exhibit multicolor fluorescence emission. With the gradual addition of $OF-I^{2+}CB[8]$ to the 1 $\mu\text{g/mL}$ aqueous solution of CDs, the fluorescence emission peak, centered on 582 nm, derived from $I^{2+}CB[8]$ increases gradually, and the fluorescence emission peak centered on 458

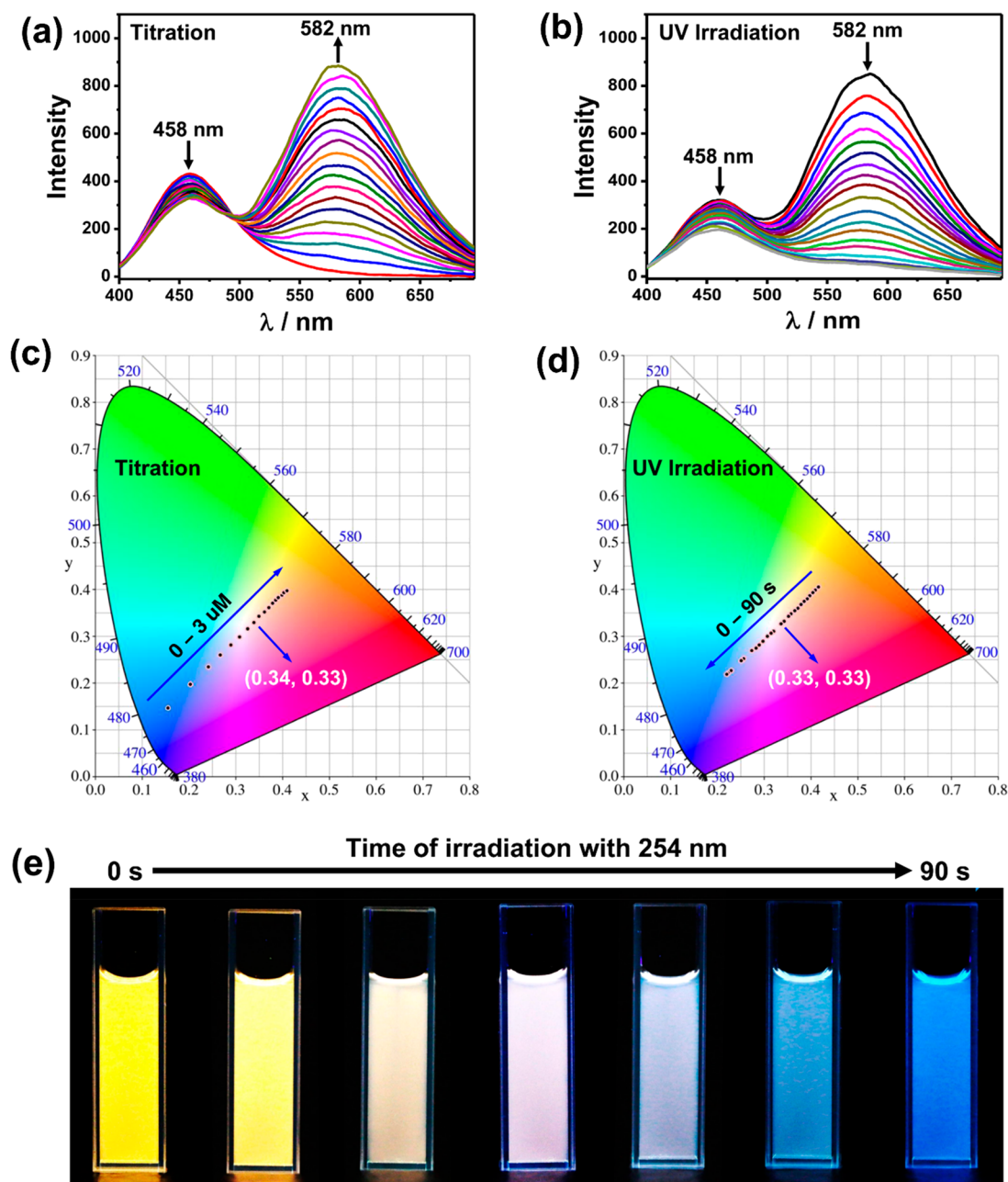


Figure 4. (a) Emission spectra of CDs ($[\text{CDs}] = 1 \mu\text{g/mL}$, $[\text{OF-1}^{2+}\text{CB}[8]] = 0\text{--}3 \times 10^{-6} \text{ M}$, $\lambda_{\text{ex}} = 360 \text{ nm}$, 298 K) with gradual addition of $\text{OF-1}^{2+}\text{CB}[8]$ in a neutral aqueous solution. (b) Emission spectral changes of $\text{CDs}@1^{2+}\text{CB}[8]$ ($[\text{CDs}] = 1 \mu\text{g/mL}$, $[\text{OF-1}^{2+}\text{CB}[8]] = 3 \times 10^{-6} \text{ M}$, $\lambda_{\text{ex}} = 360 \text{ nm}$, 298 K) upon irradiation with UV light (254 nm , 1.5 min) in a neutral aqueous solution. (c) The 1931 CIE chromaticity diagram illustrating the luminescent color changes of CDs with the gradual addition of $\text{OF-1}^{2+}\text{CB}[8]$, corresponding to (a). (d) The 1931 CIE chromaticity diagram depicting the luminescent color changes of $\text{CDs}@1^{2+}\text{CB}[8]$ upon irradiation with UV light (254 nm , 1.5 min), corresponding to (b). (e) Fluorescence photographs of $\text{CDs}@1^{2+}\text{CB}[8]$ ($[\text{CDs}] = 3 \mu\text{g/mL}$, $[\text{OF-1}^{2+}\text{CB}[8]] = 9 \times 10^{-6} \text{ M}$) with increasing the UV light (254 nm , 1.5 min) irradiation time in a neutral aqueous solution.

nm originating from the CDs undergoes (Figure 4a) a slight decrease. The fluorescence colors of the resulting ternary supramolecular assembly (Figure 4c) change linearly from bright blue to yellow, as indicated by the CIE 1931 chromaticity diagram. It is noteworthy that white-light emission (0.34, 0.33) is observed when the concentration of the $\text{OF-1}^{2+}\text{CB}[8]$ supramolecular assembly is $\sim 1.17 \mu\text{M}$. The quantum yield of the resulting white-light emission is $\sim 6.8\%$. Benefiting from the reversible photo-controlled luminescence behavior of $1^{2+}\text{CB}[8]$, the fluorescence of the resultant ternary supramolecular assembly $\text{CDs}@1^{2+}\text{CB}[8]$

can also be regulated by alternating UV and visible light irradiation. The fluorescence spectra of the $\text{CDs}@1^{2+}\text{CB}[8]$ show (Figure 4b) two emission bands centered on 458 and 582 nm, which can be ascribed to the fluorescence emissions of CDs and $1^{2+}\text{CB}[8]$, respectively. Upon irradiation of the solution with UV light (254 nm , 1.5 min), the emission peak centered on 582 nm decreases dramatically, accompanied by a slight decrease in the emission peak at 458 nm. All of the luminescence color coordinates have been calculated and plotted (Figure 4d) in the CIE 1931 chromaticity diagram, wherein the fluorescence colors of $\text{CDs}@1^{2+}\text{CB}[8]$ change

linearly from yellow to blue. The pure white-light emission (0.33, 0.33) is also realized upon UV-light irradiation for ~ 24 s, and the corresponding ratio of OF-1^{2+} to CF-1^{2+} is 32:68. The aqueous solutions of $\text{CDs@1}^{2+}\text{CCB}[8]$ exhibit (Figure 4e) colorful emissions—i.e., gold, yellow, khaki, and blue—with prolonged UV-light irradiation time. Subsequently, when the solution is irradiated with visible light (>600 nm, 30 s), the fluorescence emission of the solution returns to yellow, indicating that the fluorescence colors of $\text{CDs@1}^{2+}\text{CCB}[8]$ can be regulated efficiently by light. In control experiments, the emission peak of the binary supramolecular assembly (CDs@OF-1^{2+}) in the range of 500–700 nm is obviously weaker than that of $\text{CDs@OF-1}^{2+}\text{CCB}[8]$ (Figure S33), indicating that electrostatic interactions between the CDs and OF-1^{2+} do not effectively restrict the free rotation of C=C double bonds in OF-1^{2+} . There is no appreciable change (Figure S34) of fluorescence color when only the cationic OF-1^{2+} is gradually added to the 1 $\mu\text{g/mL}$ aqueous solution of CDs. Upon irradiation of an aqueous solution of CDs@OF-1^{2+} with UV light (254 nm, 1.5 min), there is also no appreciable change in the fluorescence color (Figure S35). These results confirm that $\text{CB}[8]$ is an indispensable component in these spectral tunable luminescent supramolecular materials. In the rational design of a supramolecular assembly with photo-responsive multicolor luminescence output, three main points need to be considered: (1) the introduction of outstanding photo-responsive components, which are indispensable for the desired photo-controlled behavior; (2) the complementary fluorescence color of fluorophores, a factor which is crucial for constructing the broad-spectrum output materials; and (3) the appropriate non-covalent bonding interactions to integrate the fluorophores. They are important in constructing the multicolor luminescence supramolecular assembly. It is believed that these design principles not only provide ideas for designing broad-spectrum-output photoluminescence materials but also serve as a reference for constructing more advanced anti-counterfeiting materials and photo-controlled molecular devices.

CONCLUSION

A photo-switched multicolor luminescent supramolecular assembly has been realized from anionic carbon dots and cationic supramolecular nanofibers that are comprised of a styrylpyridinium-modified diarylethene derivative 1^{2+} and cucurbit[8]uril. On account of the reversible photo-switchable constitutional interconversion properties of dithienylethene, the fluorescence of 1^{2+} and the binary supramolecular nanofibers can be switched on/off by alternating UV and visible light irradiation in aqueous solutions. In addition, a ternary luminescent supramolecular assembly shows multicolor fluorescence emissions, which can be interconverted efficiently in an in situ photo-controlled manner. Pure white light emission can also be realized conveniently in the photo-switched luminescence color-conversion process. These smart supramolecular luminescent materials have potential applications in the design and synthesis of anti-counterfeiting materials and photo-controlled molecular devices.

ASSOCIATED CONTENT

Supporting Information

The Supporting Information is available free of charge on the ACS Publications website at DOI: 10.1021/jacs.8b13675.

Detailed synthetic procedures, microscopic morphology, and spectroscopic (NMR, HRMS, UV–vis absorption, and fluorescence) characterization data for the guest molecules 1-2Cl and 2-Cl, CDs, supramolecular fibers ($1^{2+}\text{CCB}[8]$), and the ternary supramolecular assembly ($\text{CDs@1}^{2+}\text{CCB}[8]$), including Schemes S1 and S2, Figures S1–S35, and Tables S1–S3 (PDF)

AUTHOR INFORMATION

Corresponding Authors

*stoddart@northwestern.edu

*yuliu@nankai.edu.cn

ORCID

J. Fraser Stoddart: 0000-0003-3161-3697

Yu Liu: 0000-0001-8723-1896

Notes

The authors declare no competing financial interest.

ACKNOWLEDGMENTS

The authors thank the National Nature Science Foundation of China (NNSFC, Grant Nos. 21432004, 21672113, 21772099, and 21861132001) for financial support.

REFERENCES

- (1) (a) Zrazhevskiy, P.; True, L. D.; Gao, X. Multicolor Multicycle Molecular Profiling with Quantum Dots for Single-Cell Analysis. *Nat. Protoc.* **2013**, *8*, 1852–1869. (b) Peng, H. Q.; Niu, L. Y.; Chen, Y. Z.; Wu, L. Z.; Tung, C. H.; Yang, Q. Z. Biological Applications of Supramolecular Assemblies Designed for Excitation Energy Transfer. *Chem. Rev.* **2015**, *115*, 7502–7542. (c) Hou, X.; Ke, C.; Bruns, C. J.; McGonigal, P. R.; Pettman, R. B.; Stoddart, J. F. Tunable Solid-State Fluorescent Materials for Supramolecular Encryption. *Nat. Commun.* **2015**, *6*, 6884. (d) Ji, X.; Shi, B.; Wang, H.; Xia, D.; Jie, K.; Wu, Z. L.; Huang, F. Supramolecular Construction of Multifluorescent Gels: Interfacial Assembly of Discrete Fluorescent Gels through Multiple Hydrogen Bonding. *Adv. Mater.* **2015**, *27*, 8062–8066. (e) Wei, X.; Wu, W.; Matsushita, R.; Yan, Z.; Zhou, D.; Chruma, J. J.; Nishijima, M.; Fukuhara, G.; Mori, T.; Inoue, Y.; Yang, C. Supramolecular Photochirogenesis Driven by Higher-Order Complexation: Enantio-differentiating Photocyclodimerization of 2-Anthracenecarboxylate to Slipped Cyclodimers via a 2:2 Complex with β -Cyclodextrin. *J. Am. Chem. Soc.* **2018**, *140*, 3959–3974.
- (2) Lukinavicius, G.; Reymond, L.; Umezawa, K.; Sallin, O.; D'Este, E.; Gottfert, F.; Ta, H.; Hell, S. W.; Urano, Y.; Johnsson, K. Fluorogenic Probes for Multicolor Imaging in Living Cells. *J. Am. Chem. Soc.* **2016**, *138*, 9365–9368.
- (3) Li, S.; Peele, B. N.; Larson, C. M.; Zhao, H.; Shepherd, R. F. A Stretchable Multicolor Display and Touch Interface Using Photopatterning and Transfer Printing. *Adv. Mater.* **2016**, *28*, 9770–9775.
- (4) Pan, L.; Sun, S.; Zhang, A.; Jiang, K.; Zhang, L.; Dong, C.; Huang, Q.; Wu, A.; Lin, H. Truly Fluorescent Excitation-Dependent Carbon Dots and Their Applications in Multicolor Cellular Imaging and Multidimensional Sensing. *Adv. Mater.* **2015**, *27*, 7782–7787.
- (5) Sun, Y. Q.; Lei, Y. L.; Liao, L. S.; Hu, W. P. Competition between Arene-Perfluoroarene and Charge-Transfer Interactions in Organic Light-Harvesting Systems. *Angew. Chem., Int. Ed.* **2017**, *56*, 10352–10356.
- (6) Qasim, K.; Wang, B.; Zhang, Y.; Li, P.; Wang, Y.; Li, S.; Lee, S.-T.; Liao, L.-S.; Lei, W.; Bao, Q. Solution-Processed Extremely Efficient Multicolor Perovskite Light-Emitting Diodes Utilizing Doped Electron Transport Layer. *Adv. Funct. Mater.* **2017**, *27*, 1606874.
- (7) (a) Park, S.; Kwon, J. E.; Kim, S. H.; Seo, J.; Chung, K.; Park, S. Y.; Jang, D. J.; Medina, B. M.; Gierschner, J.; Park, S. Y. A White-Light-Emitting Molecule: Frustrated Energy Transfer between

Constituent Emitting Centers. *J. Am. Chem. Soc.* **2009**, *131*, 14043–14049. (b) Sarkar, S. K.; Kumar, G. R.; Thilagar, P. White Light Emissive Molecular Siblings. *Chem. Commun.* **2016**, *52*, 4175–4178. (c) Vandana, T.; Karuppusamy, A.; Kannan, P. Polythiophenylpyrazoline Containing Fluorene and Benzothiadiazole Moieties as Blue and White Light Emitting Materials. *Polymer* **2017**, *124*, 88–94.

(8) (a) Zhu, L.; Ang, C. Y.; Li, X.; Nguyen, K. T.; Tan, S. Y.; Agren, H.; Zhao, Y. Luminescent Color Conversion on Cyanostilbene-Functionalized Quantum Dots via In situ Photo-Tuning. *Adv. Mater.* **2012**, *24*, 4020–4024. (b) Rao, K. V.; Datta, K. K.; Eswaremoorthy, M.; George, S. J. Highly Pure Solid-State White-Light Emission from Solution-Processable Soft-Hybrids. *Adv. Mater.* **2013**, *25*, 1713–1718. (c) Aizawa, N.; Pu, Y. J.; Watanabe, M.; Chiba, T.; Ideta, K.; Toyota, N.; Igarashi, M.; Suzuri, Y.; Sasabe, H.; Kido, J. Solution-Processed Multilayer Small-Molecule Light-Emitting Devices with High-Efficiency White-Light Emission. *Nat. Commun.* **2014**, *5*, 5756. (d) Rosemann, N. W.; Eussner, J. P.; Beyer, A.; Koch, S. W.; Volz, K.; Dehnen, S.; Chatterjee, S. A Highly Efficient Directional Molecular White-Light Emitter Driven by a Continuous-Wave Laser Diode. *Science* **2016**, *352*, 1301–1304.

(9) (a) Tu, D.; Leong, P.; Guo, S.; Yan, H.; Lu, C.; Zhao, Q. Highly Emissive Organic Single-Molecule White Emitters by Engineering *o*-Carborane-Based Luminophores. *Angew. Chem., Int. Ed.* **2017**, *56*, 11370–11374. (b) Arcudi, F.; Dordevic, L.; Prato, M. Rationally Designed Carbon Nanodots towards Pure White-Light Emission. *Angew. Chem., Int. Ed.* **2017**, *56*, 4170–4173. (c) Bowers, M. J., II; McBride, J. R.; Rosenthal, S. J. White-Light Emission from Magic-Sized Cadmium Selenide Nanocrystals. *J. Am. Chem. Soc.* **2005**, *127*, 15378–15379. (d) Wu, H.; Zhou, G.; Zou, J.; Ho, C.-L.; Wong, W.-Y.; Yang, W.; Peng, J.; Cao, Y. Efficient Polymer White-Light-Emitting Devices for Solid-State Lighting. *Adv. Mater.* **2009**, *21*, 4181–4184.

(10) Zuo, M.; Qian, W.; Li, T.; Hu, X. Y.; Jiang, J.; Wang, L. Full-Color Tunable Fluorescent and Chemiluminescent Supramolecular Nanoparticles for Anti-Counterfeiting Inks. *ACS Appl. Mater. Interfaces* **2018**, *10*, 39214–39221.

(11) Po, C.; Tam, A. Y.; Wong, K. M.; Yam, V. W. Supramolecular Self-Assembly of Amphiphilic Anionic Platinum(II)Complexes: A Correlation between Spectroscopic and Morphological Properties. *J. Am. Chem. Soc.* **2011**, *133*, 12136–12143.

(12) Seki, T.; Ozaki, T.; Okura, T.; Asakura, K.; Sakon, A.; Uekusa, H.; Ito, H. Interconvertible Multiple Photoluminescence Color of a Gold(I)Isocyanide Complex in the Solid State: Solvent-Induced Blue-Shifted and Mechano-Responsive Red-Shifted Photoluminescence. *Chem. Sci.* **2015**, *6*, 2187–2195.

(13) Zhang, Q. W.; Li, D.; Li, X.; White, P. B.; Mecinovic, J.; Ma, X.; Agren, H.; Nolte, R. J.; Tian, H. Multicolor Photoluminescence Including White-Light Emission by a Single Host-Guest Complex. *J. Am. Chem. Soc.* **2016**, *138*, 13541–13550.

(14) Ni, X. L.; Chen, S.; Yang, Y.; Tao, Z. Facile Cucurbit[8]uril-Based Supramolecular Approach to Fabricate Tunable Luminescent Materials in Aqueous Solution. *J. Am. Chem. Soc.* **2016**, *138*, 6177–6183.

(15) (a) Hua, Y.; Flood, A. H. Flipping the Switch on Chloride Concentrations with a Light-Active Foldamer. *J. Am. Chem. Soc.* **2010**, *132*, 12838–12840. (b) Su, X.; Aprahamian, I. Hydrazone-Based Switches, Metallo-Assemblies and Sensors. *Chem. Soc. Rev.* **2014**, *43*, 1963–1981.

(16) (a) Chen, S.; Chen, L. J.; Yang, H. B.; Tian, H.; Zhu, W. Light-Triggered Reversible Supramolecular Transformations of Multi-Bisthiénylene Hexagons. *J. Am. Chem. Soc.* **2012**, *134*, 13596–13599. (b) Qu, D. H.; Wang, Q. C.; Zhang, Q. W.; Ma, X.; Tian, H. Photoresponsive Host-Guest Functional Systems. *Chem. Rev.* **2015**, *115*, 7543–7588. (c) Lubbe, A. S.; Liu, Q.; Smith, S. J.; de Vries, J. W.; Kistemaker, J. C. M.; de Vries, A. H.; Faustino, I.; Meng, Z.; Szymanski, W.; Herrmann, A.; Feringa, B. L. Photoswitching of DNA Hybridization Using a Molecular Motor. *J. Am. Chem. Soc.* **2018**, *140*, 5069–5076.

(17) (a) Diaz, S. A.; Menendez, G. O.; Etchelon, M. H.; Giordano, L.; Jovin, T. M.; Jares-Erijman, E. A. Photoswitchable Water-Soluble

Quantum Dots: pcFRET Based on Amphiphilic Photochromic Polymer Coating. *ACS Nano* **2011**, *5*, 2795–2805. (b) Bu, J.; Watanabe, K.; Hayasaka, H.; Akagi, K. Photochemically Colour-Tuneable White Fluorescence Illuminants Consisting of Conjugated Polymer Nanospheres. *Nat. Commun.* **2014**, *5*, 3799. (c) Irie, M.; Fukaminato, T.; Matsuda, K.; Kobatake, S. Photochromism of Diarylethene Molecules and Crystals: Memories, Switches, and Actuators. *Chem. Rev.* **2014**, *114*, 12174–12277. (d) Diaz, S. A.; Gillanders, F.; Jares-Erijman, E. A.; Jovin, T. M. Photoswitchable Semiconductor Nanocrystals with Self-Regulating Photochromic Forster Resonance Energy Transfer Acceptors. *Nat. Commun.* **2015**, *6*, 6036. (e) Diaz, S. A.; Gillanders, F.; Susumu, K.; Oh, E.; Medintz, I. L.; Jovin, T. M. Water-Soluble, Thermostable, Photomodulated Color-Switching Quantum Dots. *Chem. - Eur. J.* **2017**, *23*, 263–267.

(18) Wu, H.; Chen, Y.; Liu, Y. Reversibly Photoswitchable Supramolecular Assembly and Its Application as a Photoerasable Fluorescent Ink. *Adv. Mater.* **2017**, *29*, 1605271.

(19) (a) Foy, J. T.; Li, Q.; Goujon, A.; Colard-Itte, J. R.; Fuks, G.; Moulin, E.; Schiffmann, O.; Dattler, D.; Funeriu, D. P.; Giuseppone, N. Dual-Light Control of Nanomachines that Integrate Motor and Modulator Subunits. *Nat. Nanotechnol.* **2017**, *12*, 540–545. (b) Roke, D.; Stuckhardt, C.; Danowski, W.; Wezenberg, S. J.; Feringa, B. L. Light-Gated Rotation in a Molecular Motor Functionalized with a Dithienylene Switch. *Angew. Chem., Int. Ed.* **2018**, *57*, 10515–10519.

(20) (a) de Jong, J. J.; Lucas, L. N.; Kellogg, R. M.; van Esch, J. H.; Feringa, B. L. Reversible Optical Transcription of Supramolecular Chirality into Molecular Chirality. *Science* **2004**, *304*, 278–281. (b) Cai, Y.; Guo, Z.; Chen, J.; Li, W.; Zhong, L.; Gao, Y.; Jiang, L.; Chi, L.; Tian, H.; Zhu, W.-H. Enabling Light Work in Helical Self-Assembly for Dynamic Amplification of Chirality with Photo-reversibility. *J. Am. Chem. Soc.* **2016**, *138*, 2219–2224.

(21) Yoon, B.; Lee, J.; Park, I. S.; Jeon, S.; Lee, J.; Kim, J.-M. Recent Functional Material Based Approaches to Prevent and Detect Counterfeiting. *J. Mater. Chem. C* **2013**, *1*, 2388–2403.

(22) (a) Luo, P. G.; Sahu, S.; Yang, S.-T.; Sonkar, S. K.; Wang, J.; Wang, H.; LeCroy, G. E.; Cao, L.; Sun, Y.-P. Carbon “Quantum” Dots for Optical Bioimaging. *J. Mater. Chem. B* **2013**, *1*, 2116–2127. (b) Lim, S. Y.; Shen, W.; Gao, Z. Carbon Quantum Dots and Their Applications. *Chem. Soc. Rev.* **2015**, *44*, 362–381. (c) Hutton, G. A. M.; Martindale, B. C. M.; Reisner, E. Carbon Dots as Photosensitizers for Solar-Driven Catalysis. *Chem. Soc. Rev.* **2017**, *46*, 6111–6123.

(23) Hutton, G. A.; Reuillard, B.; Martindale, B. C.; Caputo, C. A.; Lockwood, C. W.; Butt, J. N.; Reisner, E. Carbon Dots as Versatile Photosensitizers for Solar-Driven Catalysis with Redox Enzymes. *J. Am. Chem. Soc.* **2016**, *138*, 16722–16730.

(24) Feng, T.; Ai, X.; An, G.; Yang, P.; Zhao, Y. Charge-Convertible Carbon Dots for Imaging-Guided Drug Delivery with Enhanced *in Vivo* Cancer Therapeutic Efficiency. *ACS Nano* **2016**, *10*, 4410–4420.

(25) Li, X.; Xie, Y.; Song, B.; Zhang, H. L.; Chen, H.; Cai, H.; Liu, W.; Tang, Y. A Stimuli-Responsive Smart Lanthanide Nanocomposite for Multidimensional Optical Recording and Encryption. *Angew. Chem., Int. Ed.* **2017**, *56*, 2689–2693.

(26) (a) Wang, Y.; Jiang, K.; Zhu, J.; Zhang, L.; Lin, H. A FRET-Based Carbon Dot-MnO₂ Nanosheet Architecture for Glutathione Sensing in Human Whole Blood Samples. *Chem. Commun.* **2015**, *51*, 12748–12751. (b) Bui, T. T.; Park, S.-Y. A Carbon Dot–Hemoglobin Complex-Based Biosensor for Cholesterol Detection. *Green Chem.* **2016**, *18*, 4245–4253.

(27) Cheng, H. B.; Zhang, H. Y.; Liu, Y. Dual-Stimulus Luminescent Lanthanide Molecular Switch Based on an Unsymmetrical Diaryl-perfluorocyclopentene. *J. Am. Chem. Soc.* **2013**, *135*, 10190–10193.

(28) (a) Tian, J.; Zhou, T. Y.; Zhang, S. C.; Aloni, S.; Altoe, M. V.; Xie, S. H.; Wang, H.; Zhang, D. W.; Zhao, X.; Liu, Y.; Li, Z. T. Three-Dimensional Periodic Supramolecular Organic Framework Ion Sponge in Water and Microcrystals. *Nat. Commun.* **2014**, *5*, 5574. (b) Barrow, S. J.; Kaser, S.; Rowland, M. J.; del Barrio, J.; Scherman, O. A. Cucurbituril-Based Molecular Recognition. *Chem. Rev.* **2015**, *115*, 12320–12406. (c) Fang, R.; Zhang, H.; Yang, L.; Wang, H.;

Tian, Y.; Zhang, X.; Jiang, L. Supramolecular Self-Assembly Induced Adjustable Multiple Gating States of Nanofluidic Diodes. *J. Am. Chem. Soc.* **2016**, *138*, 16372–16379. (d) Samanta, S. K.; Moncelet, D.; Briken, V.; Isaacs, L. Metal-Organic Polyhedron Capped with Cucurbit[8]uril Delivers Doxorubicin to Cancer Cells. *J. Am. Chem. Soc.* **2016**, *138*, 14488–14496. (e) Murray, J.; Kim, K.; Ogoshi, T.; Yao, W.; Gibb, B. C. The Aqueous Supramolecular Chemistry of Cucurbit[n]urils, Pillar[n]arenes and Deep-Cavity Cavitands. *Chem. Soc. Rev.* **2017**, *46*, 2479–2496. (f) Tang, X.; Huang, Z.; Chen, H.; Kang, Y.; Xu, J. F.; Zhang, X. Supramolecularly Catalyzed Polymerization: From Consecutive Dimerization to Polymerization. *Angew. Chem., Int. Ed.* **2018**, *57*, 8545–8549.

(29) (a) Li, Y.; Dong, Y.; Miao, X.; Ren, Y.; Zhang, B.; Wang, P.; Yu, Y.; Li, B.; Isaacs, L.; Cao, L. Shape-Controllable and Fluorescent Supramolecular Organic Frameworks Through Aqueous Host-Guest Complexation. *Angew. Chem., Int. Ed.* **2018**, *57*, 729–733. (b) Zhang, Y. M.; Zhang, X. J.; Xu, X.; Fu, X. N.; Hou, H. B.; Liu, Y. Rigid Organization of Fluorescence-Active Ligands by Artificial Macrocyclic Receptor to Achieve the Thioflavin T-Amyloid Fibril Level Association. *J. Phys. Chem. B* **2016**, *120*, 3932–3940.

(30) Chen, X. M.; Chen, Y.; Yu, Q.; Gu, B. H.; Liu, Y. Supramolecular Assemblies with Near-Infrared Emission Mediated in Two Stages by Cucurbituril and Amphiphilic Calixarene for Lysosome-Targeted Cell Imaging. *Angew. Chem., Int. Ed.* **2018**, *57*, 12519–12523.

(31) Feng, T.; Ai, X.; Ong, H.; Zhao, Y. Dual-Responsive Carbon Dots for Tumor Extracellular Microenvironment Triggered Targeting and Enhanced Anticancer Drug Delivery. *ACS Appl. Mater. Interfaces* **2016**, *8*, 18732–18740.

(32) Zhu, S.; Meng, Q.; Wang, L.; Zhang, J.; Song, Y.; Jin, H.; Zhang, K.; Sun, H.; Wang, H.; Yang, B. Highly Photoluminescent Carbon Dots for Multicolor Patterning, Sensors, and Bioimaging. *Angew. Chem., Int. Ed.* **2013**, *52*, 3953–3957.